Journal of Multidisciplinary Engineering Science and Technology (JMEST)
ISSN: 2458-9403
Vol. 5 Issue 10, October - 2018

Simulation and analysis of the aerodynamic forces and moments acting on the tumble flap inside an intake manifold of IC Engine

Deepak Kumar, David Chalet, Jean-François Hétet
LHEEA Lab. (ECN/CNRS)
Ecole Centrale de Nantes
Nantes, France

Vincent Raimbault, Jérôme Migaud
Advanced development
MANN+HUMMEL
Laval, France

***Abstract*— Computational Fluid dynamics is a tool widely used in automobile organization during development and optimization phase of the air intake manifold for internal combustion engines. Throttle valve, a flow control device, is extensively used in air intake lines of internal combustion engines because of their low cost, and fast operation. Nowadays, similar mechanical component close to Throttle valves are also mounted at the exits of intake manifold runners. These components referred as tumble flaps are used to guide the in-cylinder flow and hence to improve air-fuel mixing inside the combustion chamber. The movements of these flaps are controlled by the engine management system by the aid of electrical or pneumatic mechanisms. So, it becomes important to identify the torque required to move the flaps at different operating angles of the flaps. The main objective of the work is to perform CFD simulations in order to identify the forces and aerodynamic moments acting on the flaps while operating in the steady state condition. For the analysis, rhoSimpleFoam, a steady state compressible flow solver is used to simulate the 3D, steady, compressible air flow inside the intake manifold geometry. A detailed analysis of the forces and moments acting the flap has been carried out in this paper using the results of the numerical simulation.**

Later on, the prototype has been tested on the experimental flow bench to validate the results of the numerical simulation in terms of pressure drop across the component.

***Keywords*— Intake manifolds, tumble flap, aerodynamic torque**

I. INTRODUCTION

Efficient combustion and minimal emissions are a preference for both the automotive supplier and apparently for the end user as well. Design and optimization of the intake manifolds have been one of the key areas of interests of the researchers and CFD is considered as a preferred tool to minimize the cost during design and development phase on intake components [1]. One aspect of an ideal intake manifold is, to provide even distribution of the charge into each cylinder with minimal expense of pressure losses [2, 3]. The second aspect is related to length and diameter intake runners which are quite important parameters for the intake manifold tuning [4, 5, 6, 7]. The third aspect is to integrate parts at the outlet of intake runner to guide the in-cylinder flow. Tumble flaps are such devices which are installed at the outlet of the runners. Tumble flaps are used to create swirling motion alongside the cylinder axis with the aim to improve air-fuel mixing and hence to improve torque and power output. The flaps have a structure similar to throttle valves and actuated externally depending on the rotational speed and loads of the engine. Theses flap rely on an external component say electric or vacuum actuator for their movements. It raises the need to study the flow field inside and in the vicinity of the tumble flaps. The air flow impinging on the flap exerts an aerodynamic torque (TD) [8] on the flap and its direction depends on the valve geometry and its orientation. It is a common practice to express the aerodynamic torque in terms of dimensionless torque coefficients. There are two popular ways to describe the torque coefficients [8]. The classical ways where static pressure drop (ΔP) across the valve is used for the normalization. Then, the torque coefficient can be given as:

$$C_{T1} = \frac{T_D}{\Delta P d^3} \quad (1)$$

Other ways in which dynamic pressure is used for the normalization and the coefficient is defined as:

$$C_{T2} = \frac{T_D}{\frac{1}{2}\rho {V_d}^2 d^3} \quad (2)$$

Where Vd is the flow rate velocity and d is the diameter of the valve.

II. PREVIOUS WORK

Previously, many researchers have used CFD as a tool to analyze the performance of similar components like tumble flaps and closest to them is butterfly valve.

Leutwyler and Dalton [9] have performed numerical simulations to identify the performance coefficients of a

symmetric butterfly valve at various angles. They used CFX CFD code and simulated the steady flow at different pressure ratios. They have shown the importance of CFD by means of gaining valuable insight into the flow field, resulting force, and aerodynamic torque acting on the butterfly valve.

In other work, Leutwyler and Dalton [10] (using Fluent 6.0) analyzed disk pressure profile predicted by the different turbulence models and observed that realizable k-Ɛ and k-ω SST produced the best results.

Henderson et al [11] performed numerical simulation of a safety valve used in a hydro-electric power scheme using Ansys CFX 10 at various valve operating angles and estimated the hydrodynamic torque coefficients and k-ω SST for turbulence closure. They identified that flow was not able to converge properly using steady state solvers at particular valve angles due to unsteady characteristics of the flow and oscillations were observed in the residuals. Later on, better residuals were observed while simulating the flow with unsteady solvers (transient simulations).

Wang et al [12] have realized the numerical and experimental analysis of the flow taking place in a curved channel embedded with double butterfly valves (stop valve and throttle valve) and the effect of the sudden closure of the butterfly valve on the flow characteristics and the aerodynamic torque is evaluated.

III. NUMERICAL MODELLING

The numerical computation has been carried out using OpenFoam [13, 14] a finite volume [15, 16] based open source CFD code. The steady-state compressible flow solver rhoSimpleFoam [16] has been used in this work. RhoSimpleFoam is a pressure based solver based on the simple algorithm. Initially, the simple algorithm was developed for flow incompressible flows at low Mach numbers. The important development was to incorporate density and velocity correction in pressure equation such that the type of the equation changed from purely elliptic for incompressible flows to hyperbolic in transonic and supersonic compressible flows [17]. The Navier Stokes equations along with energy equation are used to describe the compressible air flow and can be written in the following form:

$$\frac{\partial \rho}{\partial t} + \nabla.(\rho u) = 0 \tag{3}$$

$$\frac{\partial(\rho u)}{\partial t} + \nabla.(\rho u u) = \underbrace{\nabla.\left\{2\mu D - \frac{2}{3}\mu(\nabla.\mathrm{u})I\right\}}_{Shear\ stress\ tensor\ \tau} - \nabla \mathrm{p} + f_b \tag{4}$$

$$\frac{\partial \rho h}{\partial t} + \nabla.(\rho u h) = \nabla.(\lambda \nabla \mathrm{T}) + \frac{\partial p}{\partial t} + u.\nabla \mathrm{p} + \sigma : \nabla \mathrm{u} \tag{5}$$

Along with the above equation, the equation of state for ideal gas is used to relate the density ρ to pressure p and temperature T (ρ=f(p,T)). It can be given as:

$$\rho = \frac{p}{RT} \tag{6}$$

Where R is gas constant.

For the turbulence closure k-ω SST has been used which provides the best results in order to calculate forces and moments [10, 11].

IV. PHYSICAL MODEL DESCRIPTION

The intake manifold is integrated part of an internal combustion engine aims to supply equal amount of charge in different cylinders. In the present study, an intake manifold designed for a four cylinder engine is used. The intake manifold has integrated tumble flaps at the outlet of each runner. In order to simplify the study, the intake manifold has been cut and single runner with flap is used for the computational analysis (Fig. 1). The pneumatic device used to control the rotation of the flap has been removed from the setup and a spring controlled mechanism has been attached to move and hold the flap at a certain angle by manual aids.

In addition to that, some plastic components (fabricated) and steel tubes are attached to the runner to provide the boundary condition in case of computational analysis and to test the component at the experimental flow bench (Fig. 2).The ultimate objective of the work is not only to identify the aerodynamic torque acting on the flap not only in the steady state but also to identify the effect of unsteady characteristics of flow such as pressure waves identified in internal combustion engine operations. So, two holes are pierced in the tested geometry for sensor installations: one to measure the pressure drop and another to measure the dynamic pressure. In the present work, the focus is to identify the forces and moments acting on the tumble flap in steady state. So, only one sensor is used to measure the pressure drop that can be seen in the Fig. 2. The pressure sensor user for the measurement has a range from 0-100 mbar with an accuracy level of ±1 mbar.

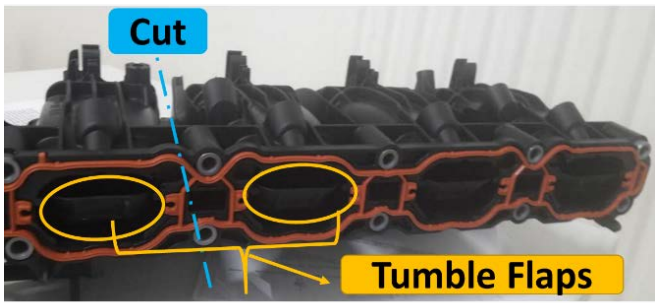

Fig. 1. *Example of a figure caption. (figure caption)*

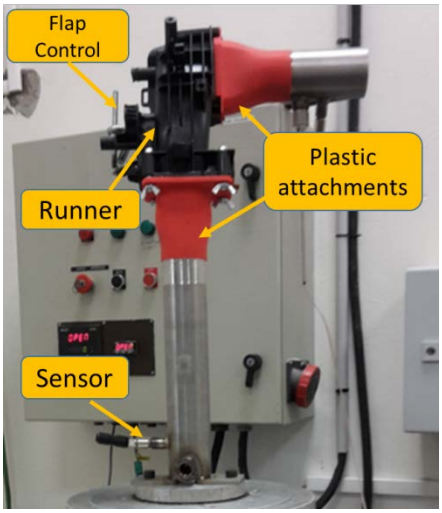

Fig. 2. *Experimental setup*

TABLE I. FLAP ANGLE AND MASS FLOW RATE

Flap Angle	Mass flow rate (kg/hr)
09.4°	100
19.4°	125
29.4°	150
39.4°	175
49.4°	200

At idle, the flaps in the intake manifold are closed. When the driver accelerates at low engine speeds, the Engine Control Unit (ECU) initiates a partial opening of the flaps. This induces a specific tumble effect as the air enters the cylinder, allowing the combustion chambers to fill more efficiently and enhancing the combustion process. At higher engine speeds the flaps are in an open position. The five mass flow rates varying between 100 kg/hr to 200 kg/hr has been chosen as the flap is opening up (Table I). The reason to choose these mass flow rates is due to a limit on the mass flow rates to be reproduced by the experimental set up of the Lab [18, 19, 20].

V. COMPUTATIONAL SETUP

The computational domain has been described in Fig. 3. Flow enters the domain through a steel tube of 50 mm diameter then passes through the flap region and exits through a circular outlet of 6 mm width (violet in color). The mesh has been created in ANSA for all the five configurations of the flaps with hexa interior method which tries to fill the main volumes with hexahedral mesh and a transition zone to the surface mesh, with a blend of tetra and pyramid elements. Every computation mesh contains around 5 million cells minutely varying from one configuration to other. The mesh density around the flap has been chosen to maintain y+ value below 1-5 for using k-ω SST turbulence model.

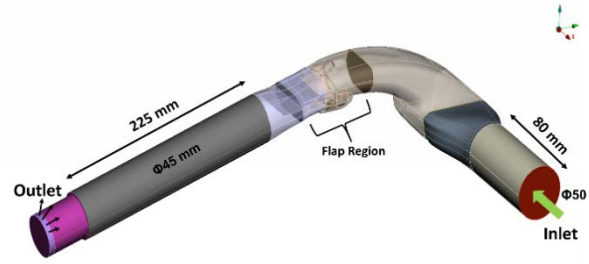

Fig. 3. *Computational domain*

The inlet boundary is defined as 'total pressure' and outlet 'mass flow rate' (which is referred as 'flowRateInletVelocity' in OpenFOAM) is specified at the outlet boundary. The idea is to further use the steady state results of this work for performing unsteady simulations by reducing the mass flow rate to zero. The turbulent kinetic energy (k) intensity of turbulence (I) has been specified at the inlet and specific dissipation rate (ω) is calculated using following equations (7) and (8).

$$\omega = \frac{C_\mu^{\frac{3}{4}} k^{\frac{1}{2}}}{l} \tag{7}$$

Where l is the mixing length giving by

$$l = 0.079\left(\frac{1}{5} d_h\right) \tag{8}$$

Calculation of the forces and moments has been performed using the function objects offered by OpenFoam 2.4. The Force Function object calculates the force and moments acting on the flap by taking into consideration of the pressure, viscous and porous effects. In the present case as there in no porous media present, so forces and moments are resultants of the first two.

VI. CONVERGENCE OF RESULTS

The accuracy of the results depends on the convergence of the solution. Residual plot is one of the criteria to realize the convergence of the computational results. Smaller the values of the residual are for a variable lesser the error in the numerical results is. But for the complex flows it is difficult to achieve lower significant low values for the residuals for each variable. Fig. 4 represents the residual plot for the fully closed position of the flap (49.4°). The important aspect to monitor convergence is to verify if the variables of interest have reached a steady solution.

To serve this purpose, variables like pressure and temperature have been monitored at a point just upstream of the flap using pressure probes function object in OpenFOAM. Fig. 5 depicts the evolution of the pressure and how it reaches the steady state solution.

It is observed while analyzing the results that the residual values get bigger as the flap is opening up,

showing the unsteady characteristics of the flow past tumble flap. The similar behavior in residuals has also been explained by Henderson et al. [11] while doing the CFD analysis of the flow past butterfly valves at different angles. So, it could be interesting to monitor the pressure downstream of the flap. Fig. 6 illustrates the static pressure plots at different flap openings and one can see waviness confirming the rise of unsteadiness in the flow past the flap.

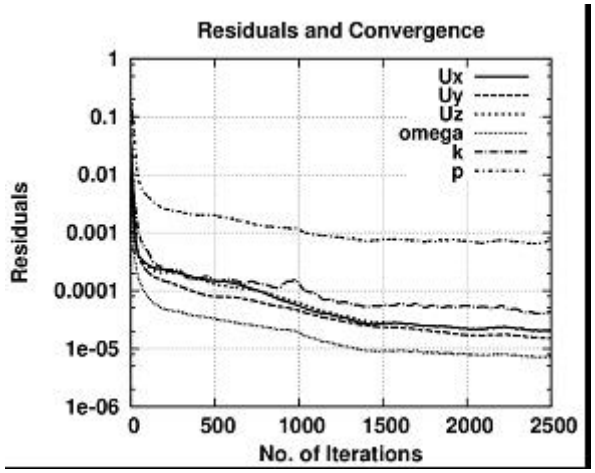

Fig. 4. *Residual plot for 49.4°*

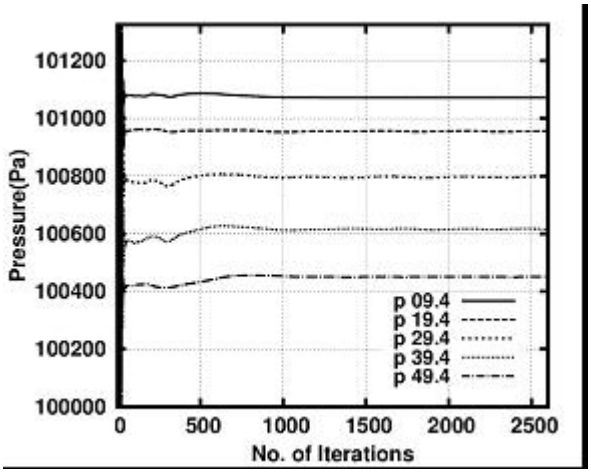

Fig. 5. *Pressure at a point upstream of flap*

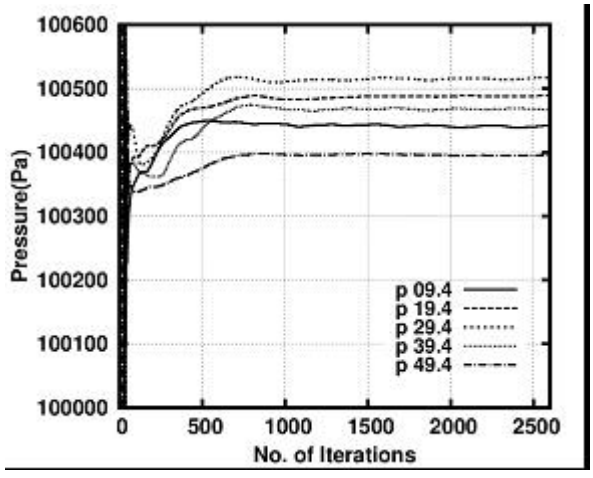

Fig. 6. *Pressure at a point downstream of flap*

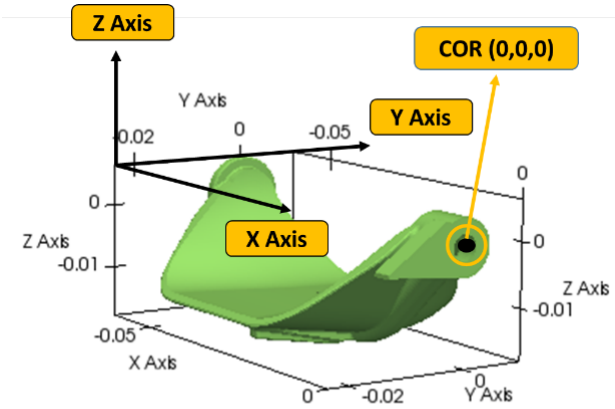

Fig. 7. *Flap coordinate system*

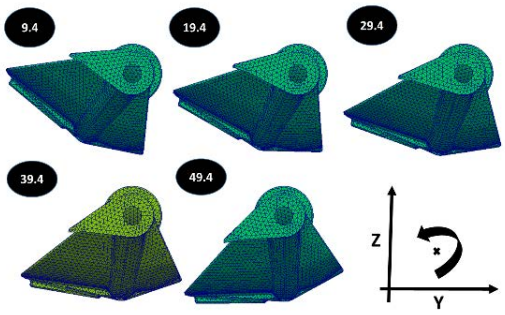

Fig. 8. *Flap orientation*

VII. Results and Discussion

Before understanding the forces and moments acting on the flap it is necessary to understand the coordinate system. The dominant flow direction around the flap will be Y axis. The moments acting on the flap are calculated around a point denoted as COR (center of rotation) in the picture below (Fig. 7) with coordinates (0, 0, 0). Fig. 8 shows the different orientations of the flap.

Forces acting on the flap are the sum of pressure and viscous forces as there is no porous medium present in the analysis. The forces along the Z axis and Y axis can also be analyzed in terms of lift and drag forces.

A. Forces

1) Fx

From the results (Fig. 10 and Table-2) it can be seen that Fx is negative and has the highest magnitude. The magnitude of the force is decreasing 11.12 to 11.03 N as the flap is opening up. So, there is not much variation (0.8%) as the neither increment in mass flow rate nor the opening of the flap will change a lot in the flow characteristics along X direction. Even though, one can observe the magnitude of the force is highest in this direction.

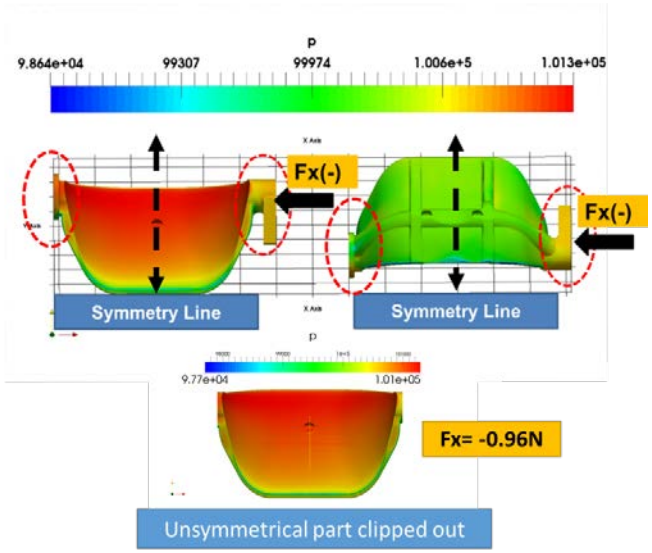

Fig. 9. *Analysis of Fx on the flap*

TABLE II. FORCES AND MOMENT ON THE FLAP

Flap Angle (degree)	Forces (N)			Moment (N-m)
	F_x	F_y	F_z	M_x
09.4°	-11.12	-0.59	-1.02	0.00333
19.4°	-11.10	-0.33	-0.89	0.00170
29.4°	-11.09	-0.14	-0.56	1.46E-05
39.4°	-11.06	-0.04	-0.18	-0.00127
49.4°	-11.02	-0.06	0.21	-0.00132

This is because of the asymmetry of the flap geometry about YZ plane. There is the symmetrical distribution of the pressure about symmetry line on both the up and down face of the flap except near the stem of the flap at both ends (Fig. 9). To analyze it, the unsymmetrical parts of the flap were clipped out as shown in the Fig. 9 and Fx was calculated with the help of Paraview. The value of the Force Fx was obtained as -0.96 N. So, the reason behind the high magnitude of the force Fx was the asymmetry of the flap geometry used in this analysis.

2) Fy

Negative Y-axis is the dominant flow direction. The force acting in Y direction is drag force. The Drag force is a function of the area perpendicular to the direction of the flow. The force acting in the Y-axis direction is decreasing in magnitude as the flap is opening up from angle 09.4° to 29.4° even though the flow rate is increasing. From the plot of the Fy (Fig. 10 and Table-2), it can be seen that force acting on the flap angle 49.4° (-0.069 N) is more than 39.4° (-0.048 N) in magnitude. This is due to the fact that projected on XZ plane or one can say area exposed to drag, is almost equal for both the flap angles which is 10.8 cm2 and 10.2 cm2 for the flap angles 39.4° and 49.4° respectively. Hence, the flow rate which is more for 49.4° causes more Fy operating on the flap

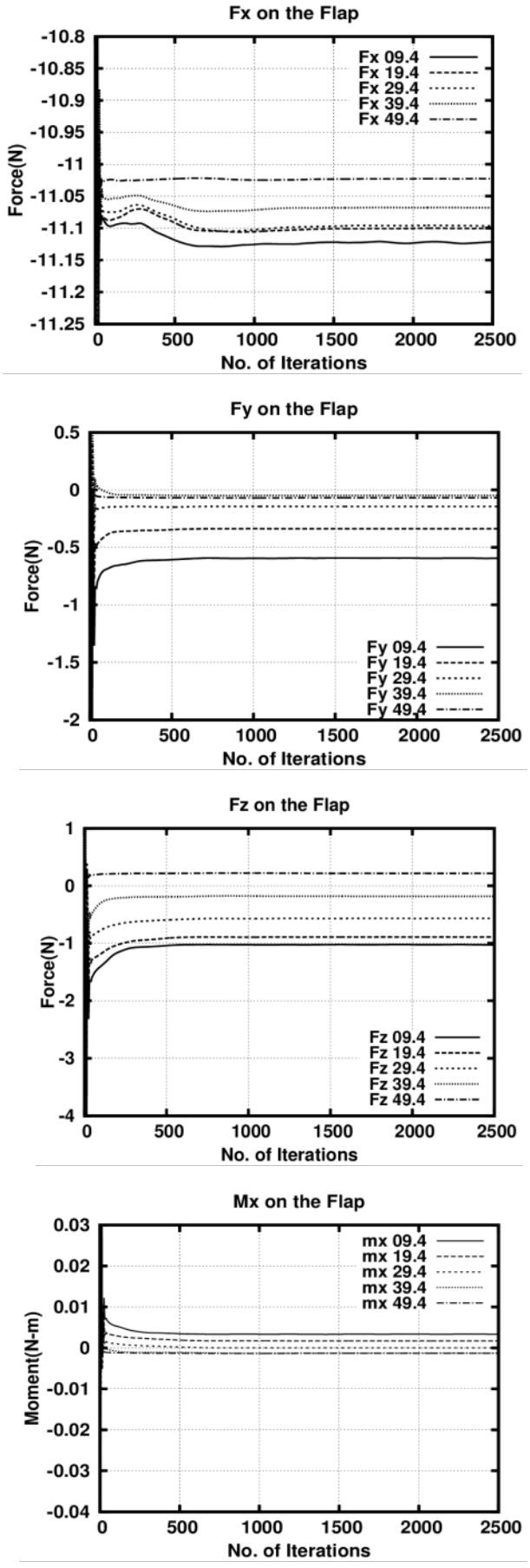

Fig. 10. *Forces and moments on different flap orientation*

3) Fz

The force acting in along Z-axis can also be called as Lift force. The variation of the force is self-explanatory and monotonous as can be seen from the Fz plot (Fig. 10 and Table-2). Initially when the Flap is at partially closed position (angle 09.4°), then a big Fz force acting on the flap in –Z axis direction which is later decreasing in magnitude and even changing its direction of action.

B. Moments

The variation of the aerodynamic moments acting on the flap can be seen in Fig. 10 and Table-2, about all the three axes. The moment (Mx) has been calculated at the point COR (0, 0, 0). As the aim of this work is to identify the moment required to turn the tumble flap so the aerodynamic moment acting action about X-axis is of topmost importance. Initially, when the flap is in partially closed condition (09.4°and 19.4°). Compressible air flow is trying to rotate the flap in the anticlockwise direction and hence the moment (Mx) has positive values (0.00333 and 0.001702 N-m). The moment reaches to almost zero when the flap orientation is 29.4° and then moment turns negative on further opening of the flap (Fig. 11).

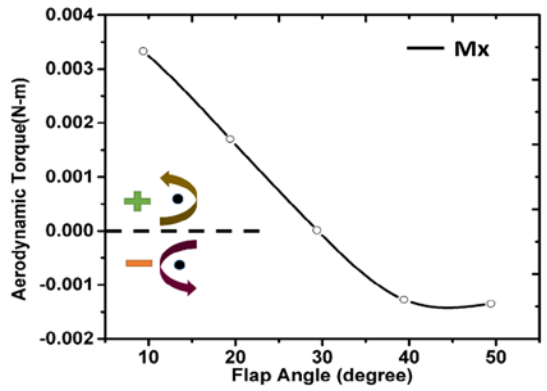

Fig. 11. *Variation of aerodynamic torque (Nm)*

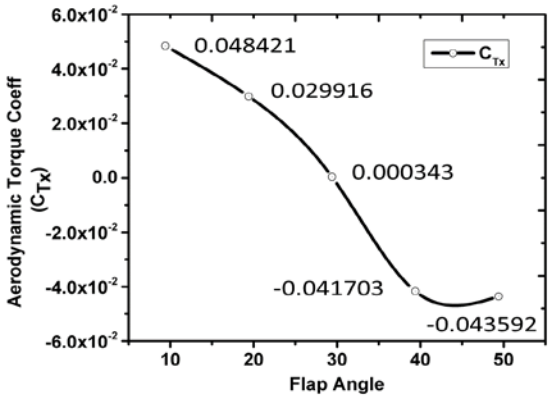

Fig. 12. *Variation of aerodynamic torque coefficient*

Aero Dynamic torque coefficient (CTx) has been identified by using (1). To calculate the torque coefficient pressure drop is estimated at two planes upstream and downstream of the flap and as the flap is asymmetric, the hydraulic diameter of the flap (0.04239 m) is utilized for the calculation (Fig. 12).

VIII. EXPERIMENTAL VALIDATION

In order to validate the simulation results, the intake runner assembly has been mounted on the Dynamic Flow bench setup. The mass flow rates according to preselected flap orientations have been reproduced at the experimental setup. As the objective of the CFD simulation is to obtain the aerodynamic torque on the flap which is not possible to be measured by the experimental means due to the small size of the geometry, low magnitude of the torque values and the complex shape of intake manifold geometry. So, validation can be performed in terms of other the pressure drop taking place inside the test component.

For this reason, a pressure drop sensor is mounted near the outlet end of the geometry to get the pressure drop value. The comparison of the simulation and experimental pressure drops in mbars can be seen in the Fig. 13 and Table-3.

The pressure drop trend suggests that for 09.4° flap orientation the major cause of the pressure loss is the flap position that is why the pressure drop is on higher side irrespective of the lower mass flow rate (100kg/hr). There are minor differences between experimental and the simulations pressure drops.

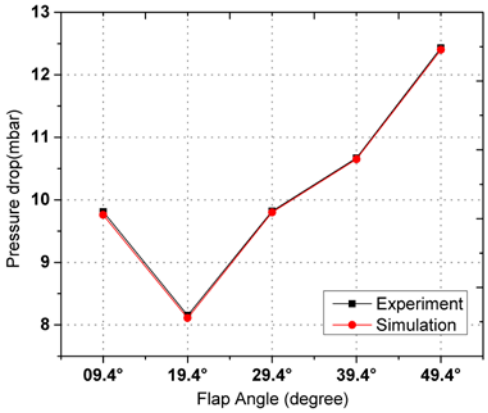

Fig. 13. *Comparison of pressure drop*

TABLE III. PRESSURE DROP COMPARISON

Flap Angle (degree)	Pressure Drop Experiment (mbar)	Pressure Drop Simulation (mbar)
09.4°	9.81	9.76
19.4°	8.15	8.11
29.4°	9.82	9.8
39.4°	10.67	10.65
49.4°	12.43	12.4

At higher mass flow rates i.e. at higher flap angles even the difference between simulation and experimental pressure drop is decreasing. The highest difference in the pressure drop is 0.05 mbar for the flap angle 09.4°.

IX. Conclusion and Perspectives

The primary aim of the work was to get aerodynamic torque acting on the flap at a fixed mass flow rate for different angles. The OpenFOAM solver rhoSimpleFoam is able to give the good insight of the flow behavior and Force and aerodynamic torque working on the flap. Therefore, rhoSimpleFoam can be used to simulate the flow inside the complex automotive components.

Another finding is that unsteadiness rises in the flow past the flap which is confirmed by placing the pressure probe downstream of the flap. The unsteadiness depends on the orientation angle of the flap. As a consequence, steady state solvers like rhoSimpleFoam find it difficult to achieve significant convergence and it is advisable to use unsteady solvers like rhoPimpleFoam for better convergence.

The aerodynamic torque (Mx) acting about X-axis is of primary importance for the automotive control point of view. The aerodynamic torque not only varies in magnitude but also in the sense of rotation. These CFD results of aerodynamic torque (Mx) can be used to identify the resultant torque required to move and maintain the flap at certain position.

From the results of the pressure drop, a good agreement is found between the simulation and the experimental results, which shows the capability of OpenFOAM to be used for complex industrial simulations.

In the current work, the forces and moment acting on the tumble flap in steady state has been calculated with help of 3D simulation. However, the flow inside the intake manifold of IC engine is highly transient. The tumble flaps are installed in a region close to the intake valves and the pressure wave propagation profoundly affects the forces and aerodynamic moments acting on the tumble flap. So, the next step is to extend the present to work in this direction. To begin with, the results from the current simulation will be used as initial solution to carry out the unsteady simulation in near future.

Acknowledgment

This work has been done as a part of international teaching and research chair entitled as “Advanced air intake systems and thermal management” between MANN+HUMMEL and Ecole Centrale de Nantes.

References

[1] D. Pai,H.S. Singh and P.V. Fayaz Muhammed, "Simulation based approach for optimization of intake manifold," SAE Technical Paper 2011-26-0074, 2011

[2] K. V. Tallio and B. J. Tobis, "The application of steady-flow loss correlations to intake manifold design," SAE Technical Paper 930608, 1993

[3] William Taylor III, James H. Leylek, and Le T. Tran "Advanced computational methods for predicting flow losses in intake regions of diesel engines," SAE Technical Paper 970639, 1997

[4] A. Ohata, Y. Ishida,”Dynamic inlet pressure and volumetric efficiency of four cycle four cylinder engine”, SAE Technical Paper 820407, 1982

[5] M.A. Ceviz, M. Akin, “Design of new SI engine intake manifold with variable length plenum”, Energy Conversion and Management
Volume 51, Issue 11, 2239–2244,2010

[6] D.E. Winterbone, R.J. Pearson, “Design techniques for engine manifolds - Wave action methods for IC Engines”, Professional Engineering Publishing Limited London and Bury st Edmunds, UK, 1999.

[7] D.E. Winterbone, R.J. Pearson, “Theory of engine manifold design - Wave action method for IC Engines, Professional Engineering Publishing Limited London and Bury st Edmunds, UK, 2000.

[8] C. Solliec and F. Danbon, “Aerodynamic torque acting on a butterfly valve comparison and choice of a torque coefficient”, ASME Journal of Fluids Engineering, Volume 121, 1999

[9] Z. Leutwyler and C. Dalton, A “Computational study of torque and forces due to compressible flow on a butterfly valve disk in mid-stroke position”, ASME Journal of Fluids Engineering, Volume 128, 1074–1088, 2006

[10] Z. Leutwyler and C. Dalton, “A CFD study of the flow field, resultant force, and aerodynamic torque on a symmetric disk butterfly valve in a compressible fluid”, ASME Journal of Pressure Vessel Technology, Volume 130, 2008

[11] A. D. Henderson, J. E. Sargison, G. J. Walker and J. Haynes, “A numerical study of the flow through a safety butterfly valve in a hydro-electric power scheme”, 16th Australasian Fluid Mechanics Conference Crown Plaza, Gold Coast, Australia 2-7 December 2007

[12] P. Wang , Y. Liu, Z. Hu, S. Xu, “Rapid close of a butterfly valve placed in a curved channel: a computational study of unsteady steam flow and aerodynamic torque”, Proceedings of ASME Turbo Expo 2016: Turbomachinery Technical Conference and Exposition

[13] OpenFoam User guide, OpenFoam

Foundation,2016
[14] OpenFoam Programmers guide ,2016
[15] J.D. Anderson, “Computational fluid dynamics - the basics with applications”, McGraw-Hill, 1976
[16] J. H. Ferziger, M. Peric,” Computarional methods for fluid dynamics”, Springer, ISBN 3-540-42074-6, 2002
[17] F. Moukalled ,L. Mangani, M. Darwish ,”The Finite Volume Method in Computational Fluid Dynamics”, Fluid Mechanics and Its Applications, Volume 113,2016
[18] D. Chalet, A. Mahé, J.F. Hetet, J. Migaud, “A new modeling approach of pressure waves at the inlet of internal combustion engines” Journal of Thermal Science, Volume 20, n°2, pp. 181-188, 2011
[19] H. Mezher, D. Chalet, J. Migaud and P. Chesse, "Frequency based approach for simulating pressure waves at the inlet of internal combustion engines using a parameterized model," Applied Energy, vol. 106, pp. 275-286, 2013.
[20] D. Chalet, A. Mahe, J. Migaud and J. F. HETET, "Multi-frequency modelling of unsteady flow in the inlet manifold of an internal combustion engine," Journal of Automobile Engineering, vol. 226, no. 5, pp. 648-658, 2012.

NOMENCLATURE / SYMBOLS

C_{T1}	Aerodynamic Torque coefficient
C_{T2}	Aerodynamic Torque coefficient
C_{Tx}	Aerodynamic Torque coefficient for torque about x axis
C_{μ}	k-ω SST turbulence model constant
D	Deformation rate tensor
d_h	Hydraulic diameter (m)
d	Diameter of the valve (m)
f_b	Body forces
h	Specific enthalpy (kJ/kg)
k	Turbulent kinetic energy (m^2/s^2)
l	Mixing length (m)
m_i	Moment about *i* axis (N-m)
p	Absolute pressure (Pa)
ΔP	Static pressure drop
P_d	Dynamic pressure (Pa)
R	Specific Gas constant (KJ/kg-K)
T	Temperature (K)
T_D	Aerodynamic Torque (N-m)
u	Velocity vector
V_d	Flow rate velocity (m/s)
y+	Dimensionless normal distance from wall

GREEK LETTERS

Λ	Thermal diffusivity
M	Dynamic viscosity (kg/m-s)
P	Density of air(kg/m^3)
Σ	Cauchy stress tensor
τ	Shear stress tensor
ω	Specific dissipation rate (1/s)

ABBREVIATIONS

CFD	Computational Fluid Dynamics
COR	Centre Of Rotation
ICE	Internal Combustion Engine
SST	Shear Stress Transport
ECU	Engine Control Unit